

Article

Nano-Functionalized Magnetic Carbon Composite for Purification of Man-Made Polluted Waters

Tetyana I. Melnychenko ^{1,*} , Vadim M. Kadoshnikov ¹ , Oksana M. Arkhipenko ¹ , Tetiana I. Nosenko ² , Iryna V. Mashkina ² , Lyudmila A. Odukalets ¹ , Sergey V. Mikhlovsky ^{3,4}  and Yuriy L. Zabulovov ¹

- ¹ State Institution "The Institute of Environmental Geochemistry of National Academy of Sciences of Ukraine" (NASU), Academician Palladin Avenue, 34a, 03142 Kyiv, Ukraine; zabulovov@nas.gov.ua (Y.L.Z.)
² Department of Computer Science, Faculty of Information Technologies and Mathematics, Borys Grinchenko Kyiv Metropolitan University, Bulvarno-Kudriavskaya Str., 18/2, 04053 Kyiv, Ukraine
³ Advanced Nanostructured Materials Design and Consultancy (ANAMAD) Ltd., Sussex Innovation Centre Science Park Square, Falmer, Brighton BN1 9SB, UK; sergeymikhlovsky@gmail.com
⁴ Chuiko Institute of Surface Chemistry of NASU, 17, General Naumov Str. (Oleg Mudrak), 03164 Kyiv, Ukraine
 * Correspondence: sgns_melnichenko@nas.gov.ua

Abstract

Among the main man-made water pollutants that pose a danger to the environment are oil products, heavy metals, and radionuclides, as well as micro- and nanoplastics. To purify such waters, it is necessary to use advanced methods, with sorption being one of them. The aim of this work is to develop a nano-functionalized composite, comprising magnetically responsive, thermally expanded graphite (TEG) and the natural clay bentonite, and to assess its ability to purify man-made contaminated waters. Throughout the course of the research, the methods of scanning electron microscopy, optical microscopy, dynamic light scattering, radiometry, and atomic absorption spectrophotometry were used. The use of the TEG–bentonite composite for the purification of the model water, simulating radioactively contaminated nuclear power plant (NPP) effluent, reduced the content of organic substances by 10–15 times, and the degree of extraction of cesium, strontium, cobalt, and manganese was between 81.4% and 98.8%. The use of the TEG–bentonite composite for the purification of real radioactively contaminated water obtained from the object "Shelter" ("Ukryttya" in Ukrainian), in the Chernobyl Exclusion Zone, Ukraine, with high activity, containing organic substances, including micro- and nanoplastics, reduced the radioactivity by three orders of magnitude. The use of cesium-selective sorbents for additional purification of the filtrate allowed for further decontamination of radioactively contaminated water with an efficiency of 99.99%.

Keywords: TEG–bentonite composite; magnetically responsive expanded graphite; bentonite; micro- and nanoplastics; oil pollution; radionuclides; sorption



Academic Editor: Giuseppe Cirillo

Received: 8 September 2025

Revised: 6 October 2025

Accepted: 10 October 2025

Published: 13 October 2025

Citation: Melnychenko, T.I.; Kadoshnikov, V.M.; Arkhipenko, O.M.; Nosenko, T.I.; Mashkina, I.V.; Odukalets, L.A.; Mikhlovsky, S.V.; Zabulovov, Y.L. Nano-Functionalized Magnetic Carbon Composite for Purification of Man-Made Polluted Waters. *C* **2025**, *11*, 77. <https://doi.org/10.3390/c11040077>

Copyright: © 2025 by the authors. Licensee MDPI, Basel, Switzerland. This article is an open access article distributed under the terms and conditions of the Creative Commons Attribution (CC BY) license (<https://creativecommons.org/licenses/by/4.0/>).

1. Introduction

Man-made or anthropogenic pollution, including water pollution caused by various human activities, has a profound impact on the environment. The priority pollutants of water bodies in Ukraine are oil products, heavy metals, and radionuclides, as well as micro- and nanoplastics, due to the widespread use of polymeric materials [1–3].

The main source of radioactive pollution in this country originates from the Chernobyl Nuclear Power Plant (NPP) catastrophe, which occurred in 1986, but due to its large scale, remains a threat to the environment and human health today [2,4]. In general,

anthropogenic radioactive contamination of water could be caused by emissions from NPPs, mining, medical diagnostics and radiotherapy, and nuclear accidents such as those occurred in Chernobyl and Fukushima-Daiichi NPPs [5]. Decontamination and disposal of nuclear waste is a huge problem. The Chernobyl accident generated high volumes of liquid radioactive waste (LRW), which is stored in specially built “temporary” subsurface storage facilities disposing of low- and intermediate-level radioactive wastes. LRW can come from different sources [6], and depending on the source and pre-treatment, they have a complex composition, including surfactants, large and small organic molecules, chelating agents such as EDTA, and colloid particles. Microplastics are not usually expected to be present in nuclear wastewater, but in fact, polymer gels and foams are used to clean surfaces from radioactive contamination [7] and polymer emulsions are sprayed over contaminated surfaces to create a film that suppresses radioactive dust formation [8].

Highly dispersed micro- and nano-sized microplastic particles are formed in the process of destroying polymeric materials that are abundantly present as contaminants in water, under the influence of sunlight and other environmental factors. Micro- and nanoplastics can adsorb and accumulate foreign toxic substances: in particular, persistent organic pollutants, such as polycyclic aromatic hydrocarbons and organochlorine pesticides [9,10]. Due to their small size, large surface area, and hydrophobic properties, microplastics are also able to actively adsorb radionuclides and other heavy metals [11]. Moreover, microplastics can contribute to the spreading of radioactive contamination, due to this ability to adsorb and retain radionuclides [12].

The mechanism by which radionuclides are bound to microplastics is determined by their surface properties, particle size, and the surrounding environment [10]. The adsorption capacity of microplastics for various radionuclides differ. In natural waters, microplastic pollution is often accompanied by oil pollution, as the former are essentially the product of oil processing [13]. A common feature of microplastics and oil products, such as solvents and extraction agents, is their hydrophobicity. In addition, oil products and spills, due to their low solubility, often form a stable dispersion/emulsion in water, particularly in the presence of surfactants.

To clean systems that contain microplastics, membrane technologies such as ultrafiltration and reverse osmosis are used; the disadvantages of these are considered to be their low permeability, reduced filtration rate, and fouling and membrane contamination [14]. Membrane technologies could also be used to separate oil from water [15]. To increase the efficiency of separation, nanofibrous composite membranes have been designed based on polymer nanofibers of polyvinylidene fluoride modified by treatment with alkalis, biosurfactants, TiO_2 , and CuO particles. As a result of these amphiphilic biosurfactants combined with metal oxides, the surface energy was reduced and, therefore, the adsorption of micro- and nanoplastics was enhanced, preventing membrane fouling, increasing the efficiency of filtration and the separation of oil and water [16].

High hydrophobicity of both oil and nanoplastics leads to the formation of conglomerates; for the removal of these, it is advisable to use the sorption method, using sorbents that include nanostructured elements. Such sorbents are characterized by a high specific surface, the possibility of modification and regeneration, ease of processing, and disposal. The most promising among them are carbon nanostructured sorbents: in particular, sorbents based on thermally expanded graphite (TEG).

To obtain TEG, intercalated/oxidized graphite is used. Compounds that form gaseous substances as a result of thermal shock, and, thus, break the bonds between the graphene layers of graphite, are used as intercalants. In the presence of oxidizers, oxidation of the graphite/graphene surface occurs simultaneously with expansion, which leads to a significant improvement in their sorption properties. Thus, fragments of oxidized graphene are

always present in the structure of the TEG. In fact, graphite thermal exfoliation/expansion of graphite is often used as the starting point for the synthesis of graphene oxide. The most well-known protocols of synthesis are Brodie's and Hummers' methods and their modifications, in which KClO_3 and fuming HNO_3 (original Brodie method) or NaNO_3 , KMnO_4 , and concentrated H_2SO_4 (original Hummers' method) are used [17]. Various other oxidizing reagents and pretreatment procedures are used in a modified version of Hummers' method [18].

Thermally expanded graphite effectively retains absorbed oil due to its well-developed porous structure and hydrophobicity, which depend on the degree of its expansion [19]. The sorption capacity of TEG is affected by the size of the capillary gaps in the expanded part of the material [20]. The mechanism of hydrocarbon absorption by TEG includes the pore-filling effect, π - π conjugation, and electrostatic interaction [21].

In addition to a high sorption capacity for oil products, TEG-based sorbents are characterized by a moderate affinity for heavy metals. There are two main reasons for this affinity. Firstly, the degree of stratification leading to a porous structure affects the sorption capacity and affinity of some metals to interact with Van der Waals forces in crystalline structures, since metal ions may be "captured" by smaller cavities. Secondly, the oxidation of graphene layers in the graphite structure causes its chemical functionalization, creating a range of oxygen-containing groups, which could form surface complex compounds with metal ions [20]. Like any other oxidized carbon material, GO and EG also possess cation exchange properties, mainly due to the presence of acidic functional groups such as $-\text{COOH}$ and $-\text{SO}_3\text{H}$; the latter is due to the use of sulfuric acid in their preparation [22].

The mechanism of the formation of graphene oxide (GO) and the chemical bond between oxidized graphene and metal cations has not been fully elucidated. In general, the efficiency of binding metal cations to GO increases with increasing ionic charge and depends on their ability to form coordination-covalent bonds with the oxygen groups of GO. Graphene oxide contains two different types of binding sites. It was found that trivalent cations (Gd^{3+} , Lu^{3+} , Ga^{3+}) were adsorbed stronger than divalent cations (Mn^{2+} , Sr^{2+} , Ca^{2+}), and monovalent alkali metal cations were weakly adsorbed and could not replace higher-charged cations from GO. The ions of the same charge with larger radii that were capable of forming covalent coordination compounds were more efficiently adsorbed ($\text{Gd}^{3+} > \text{Ga}^{3+}$, $\text{Mn}^{2+} > \text{Sr}^{2+} > \text{Ca}^{2+}$, $\text{Cs}^+ > \text{Na}^+$). The vast majority of existing carboxyl groups in GO are located in tiny defects with several carbon atoms and vacancies on the main planes. The density of these defects with vacancies was estimated as being one per every 200 carbon atoms. Thus, oxidized graphene effectively chelates metal cations, reliably protecting them from hydrolysis [23].

The affinity of a metal cation to the surface of a carbon matrix is determined not only by the properties of the carbon matrix, but also by the physicochemical properties of the sorbate. Coetzee et al. [20] showed that transition metals (manganese, molybdenum, copper, etc.) were capable of forming coordination bonds with the graphene matrix, whereas alkaline earth metals (calcium and strontium) are sorbed almost completely. The relatively low affinity of alkali metals to a graphene matrix is probably due to the fact that the main mechanism of their sorption is ion exchange, and their ability to form surface complexes is low.

Natural ion exchangers, highly dispersed layered aluminosilicates of the structural type (2:1) such as smectite clay minerals, have a significantly higher affinity for metal cations and a much higher ion exchange capacity than carbon materials [24]. In practice, bentonite is used to purify man-made contaminated water, including radioactive wastewater [25]. The ability of bentonite to sorb radionuclides and heavy metal ions from low-concentration solutions or natural waters is due to the nature of the active centers on the outer surface of

montmorillonite (the main constituent of bentonite) nanocrystals, which are represented by aluminol ($>\text{Al}-\text{OH}$) and silanol ($\equiv\text{Si}-\text{OH}$) groups and/or their Na forms [26]. In addition, active centers are located on the surface of montmorillonite nanocrystals, caused by the negative charge associated with isomorphic substitutions of silicon (Si^{4+}) in the tetrahedral layer for Al^{3+} or Fe^{3+} ions and/or substitution of Al^{3+} in the octahedral layer for Fe^{2+} or Mg^{2+} ions. In addition to the hydrophilic centers, a small number of hydrophobic centers are localized on the basal surfaces of microcrystals, providing the affinity of such crystals to non-polar hydrocarbons. It should be noted that the hydrophilicity of clay minerals, particularly montmorillonite, significantly exceeds their hydrophobicity, which determines the preferential use of clay minerals for the sorption of cations and hydrophilic organic substances. The surface charge (zeta potential), which depends on the concentration of electrolytes in the dispersion medium, is important for sorption processes [27–29].

The properties of montmorillonite can be changed by mechanical activation. In the process of tribochemical treatment, two main stages can be distinguished. The first is the destruction of particles by an external force, usually acting on their totality. The second is the aggregation of particles, both spontaneous and caused by external forces. Both processes—destruction and aggregation—significantly depend on the nature of the external environment and the conditions of its interaction with the particles. At the first stage, partial fragmentation of the crystal into separate fragments occurs, which can retain the original structure or transform into an amorphous state. Many fragments participate in the process simultaneously. Crushing into fragments occurs randomly, and the number of fragments is also random [30].

Together with fragmentation and aggregation, a change in the crystal structure and energy state of the surface layers of particles occurs during the treatment. In the thermodynamic approach, the surface layer is considered as a surface. According to thermodynamic theory, the surface charges of the contacting systems are located on this plane. This representation is idealized, since the charges are separated by a certain distance equal to the thickness of the surface layer (the so-called double electric layer). The structure and physical properties of the surface layer existing at the boundary between two media are different from those in these media [31]. The state of the surface layer has a significant effect on the interaction of particles with each other and with the medium. For nanoparticles, due to the relatively developed phase boundary, the influence of the medium is especially significant. Under intense mechanical action, new active centers of different natures are formed on the surface of crystals, which is of decisive importance for the self-organization and sorption processes. In cases where chemical adsorption is accompanied by dissociation of the active center into ions and atoms, a certain activation energy is required for its implementation, which is determined not only by the mechanism of the elementary act of destruction, but also by the nature of the adsorption centers [30]. Selective mechanochemical activation of bentonite improves the quality of resulting composites [32].

It has been established that mechanical activation of graphite materials, which causes a change in the double electric layer, leads to the formation of a large number of active acid centers on their surface. The composition and concentration of functional groups determine such surface properties as hydrophilicity and potential, which actively affects sorption properties. After mechanical activation of graphite materials, an increase in the number of functional groups is observed. Brønsted acid centers appear due to the oxidation of both existing groups and the side faces of ground graphite crystals [33].

As a result of mechanical activation of bentonite in combination with activated carbon, a bentonite–carbon composite was obtained. Improvement of the sorption properties of the composite, relative to tetracycline hydrochloride and triphenylmethane dye brilliant green, was noted, which was due to the formation of additional centers. At the same time,

partial destruction of silanol bonds and, accordingly, a decrease in ion-exchange properties occurred, as evidenced by a decrease in the intensity of the 1630 cm^{-1} band in the IR spectrum of this composite [34,35]. Considering that the composition of thermally expanded graphite contains layers of oxidized graphene and nanostructured elements, replacing activated carbon with TEG could improve the sorption properties of bentonite-based composites. The introduction of a magnetic component (magnetite, metallic iron, etc.) into the TEG composition would significantly simplify the sorbent recovery, using magnetic separation.

Thus, despite the high demand for means and methods for purifying multiphase and multicomponent man-made contaminated waters, including liquid radioactive waste, it is quite difficult to select a universal sorbent. Considering the functional properties of magnetically responsive TEG, which has a high affinity for non-polar hydrocarbons and microplastics, as well as the high hydrophilicity of highly dispersed aluminosilicates, the aim of this work was to develop a nano-functionalized composite based on magnetically responsive TEG and bentonite, and study its application for the purification of multiphase and multicomponent man-made contaminated waters.

2. Materials and Methods

2.1. Materials

High purity natural graphite with low ash content obtained from Zavalyvskiy Graphite Ltd. (Gajvoron district of Kirovograd region, Ukraine), was intercalated with concentrated (95%) sulfuric acid, according to the method described by Nasiedkin et al. [36]; the graphite was treated with concentrated sulfuric acid at $20 \pm 5\text{ }^{\circ}\text{C}$ for 1 h in the presence of an oxidizer, ammonium persulfate $(\text{NH}_4)_2\text{S}_2\text{O}_8$, at the mass ratio: $\text{C}:\text{H}_2\text{SO}_4:(\text{NH}_4)_2\text{S}_2\text{O}_8 = 1.0:2.0:0.7$. The intercalated graphite was washed with distilled water to pH 6 and dried at a temperature of $40 \pm 5\text{ }^{\circ}\text{C}$ for 6 h.

A magnetoresponsive sorbent was prepared by combining intercalated graphite with micro- and nanoparticles (size from 0.1 to $100\text{ }\mu\text{m}$) of the magnetoresponsive component comprising metallic iron and iron oxides; the latter were obtained by the plasma-chemical method described by Kadoshnikov et al. [19]. A sample of graphite intercalated with sulfuric acid, as described above, was mixed with micro- and nanoparticles at the mass ratios from (1:1) to (1:3) using a UOSLab SH 3 laboratory shaker (Ukrorgsyntez Ltd., Kyiv, Ukraine). After thorough mixing for 20 min, at 400 rev/min, the mixture was exposed to microwave radiation (microwave oven MS23K3614AW/BW-SAMSUNG, Kuala Lumpur, Malaysia, power 800 W) for 30 s.

Bentonite clay, grade P4T2K (Dash-Bent JSC, Cherkasy region, Ukraine), containing at least 70% montmorillonite, with a particle size of no more than $100\text{ }\mu\text{m}$, was used as received.

Oil samples were supplied by the Nadvirna Oil Refinery (Naftokhimik Prykarpattia JSC, Nadvirna, Ukraine), from an oil field in the Western Ukrainian region. Its parameters were as follows: low density (848.1 kg/m^3), sulfur content (0.53%), water (0.11%) and mechanical impurities (0.008%), boiling starting point $-50\text{ }^{\circ}\text{C}$, pour point $+9\text{ }^{\circ}\text{C}$, and viscosity above $70\text{ }^{\circ}\text{C}$ is 4.22 St [37].

2.2. Obtaining Magnetoresponsive TEG–Bentonite Composite

The magnetically responsive TEG prepared as described above was mixed with highly dispersed bentonite in a weight ratio between 1:5 and 1:50, followed by gentle mechanical activation of the mixture for 30 min using a UOSLab SH 3 laboratory shaker.

2.3. Characterization Methods

The particle size distribution of bentonite was determined by the dynamic light scattering method, using a Mastersizer 2000 laser sedimentograph with a HydroS liquid dispersion module (Malvern Instruments Ltd., Malvern, UK); the operating principle of this is based on laser diffraction of light. Particles in a parallel laser beam scatter light at a constant angle, the value of which depends on their diameter. The measurement range is 0.02–2000 microns.

The topographic features of the TEG–bentonite composite components (magnetoresponsive TEG and bentonite) were studied by scanning electron microscopy (SEM), using a field emission scanning electron microscope JSM-6700F (JEOL, Akishima, Japan). Optical microscopy (Bresser LCD MICRO 5 mp, Bresser, Germany) was used to study the topographic features of the obtained TEG–bentonite composite. The optical properties of the composite (powder placed on a glass slide) were studied in reflected light without the use of binders.

The content of organic substances in solutions was estimated by measuring the chemical oxygen demand (COD) using a dichromate oxidizability method [38].

The content of cesium, strontium, cobalt, and manganese ions in the original model solution and after purification was determined by the atomic absorption spectroscopy (AAS) method, using an atomic absorption spectrophotometer AA-8500 (Nippon Jarrell-Ash (Co., Ltd., Uji City, Kyoto, Japan).

The activity of gamma-emitting radionuclides in the original radioactively contaminated water and after purification was determined using a CANBERRA gamma spectrometric complex (Canberra Industries, Inc., Meriden, CT, USA). The activity of ^{90}Sr was determined by β -radiometric measurements after radiochemical extraction using a UMF-1500 (Research Center for Multilevel Measurements, Moscow Russian Federation) low-background beta radiometer and a RUB-01P radiometer (measurements were carried out at the Institute for Safety Problems of Nuclear Power Plants of NASU, Kyiv, Ukraine).

2.4. Study of the Sorption Activity of the TEG–Bentonite Composite

A model solution simulating the composition of the radioactive wastewater from Ukrainian NPPs was used to study the sorption properties of the obtained TEG–bentonite composite.

Samples of real radioactively contaminated wastewater were obtained from the Shelter Storage Facility, Chernobyl Exclusion Zone, Ukraine.

2.4.1. Model Solution—Simulant of Radioactively Contaminated Water of Nuclear Power Plants

The model (nonradioactive) aqueous solution contained the following:

- Stable isotopes of radionuclides—cesium (10.2 mg/dm^3), strontium (10.9 mg/dm^3), cobalt (4.2 mg/dm^3), and manganese (2.4 mg/dm^3); they were used as nitrates (KhimLaborReaktiv, Brovary, Kyiv region, Ukraine).
- Organic substances—oxalic acid (65 mg/dm^3); citric acid (10 mg/dm^3); the decontamination surfactant “SHCHIT K” (Shield in Ukrainian, 180 mg/dm^3 , “Energokhim”, Kyiv, Ukraine), which is used for decontamination of workwear, equipment, and premises at nuclear power plants in Ukraine; sodium salt of ethylenediaminetetraacetic acid (KhimLaborReaktiv, 100 mg/dm^3); shampoo/soap (150 mg/dm^3); universal washing powder «Lotus» (10 mg/dm^3); and oil (200 mg/dm^3).
- Inorganic substances—boric acid (1200 mg/dm^3), sodium hydroxide (1040 mg/dm^3), potassium hydroxide (90 mg/dm^3), and nitric acid (400 mg/dm^3), KhimLaborReaktiv, Brovary, Kyiv region, Ukraine.

pH of the model solution was ≈ 9.1 , total salt content 3.4 g/dm^3 , and COD $1500 \text{ mgO}_2/\text{dm}^3$.

The composition and concentration of the ingredients mimic the real radioactive wastewater obtained from different sources in the radioactivity decontamination at NPPs. All chemical reagents used were of analytical grade.

2.4.2. Radioactively Contaminated Water

A sample of radioactively contaminated water (RCW) was collected at the object “Ukryttya” (Chernobyl Exclusion Zone, Ukraine). The radionuclide composition of the RCW was as follows: ^{137}Cs — 3.3×10^7 , ^{90}Sr — 4.9×10^6 , ^{154}Eu — 2.4×10^3 , and ^{241}Am — 2.2×10^4 Bq/dm³. In addition to radionuclides, the waters of the “Ukryttya” facility contained hydrophobic polymeric compounds used as a component of dust suppression solutions (siloxane acrylates), the non-ionic surfactant OP-7 (a reaction product of a mixture of mono- and dialkylphenols with ethylene oxide, used as an emulsifier), glycerol, oxalic acid, oleic and oxyethylene diposphonic acids, and ethyl alcohol [39]. The radioactively contaminated water of the object “Ukryttya” also included micro- and nanoplastics, which were formed as a result of the aging and destruction of paint coatings; on the surface of these, so-called “condensation radiocesium” was sorbed as a result of the Chernobyl NPP accident. Radionuclides in a dissolved state are partially sorbed on particles of micro- and nanoplastics, significantly increasing the activity of the solid phase. The combination of surfactants, micro- and nanoplastics, siloxane acrylate latexes, and oil contaminants in the presence of stabilizers leads to the formation of kinetically stable colloids or pseudocolloids, for which the Tyndall effect is observed: a phenomenon of light-scattering by colloidal particles, manifested as a visible luminous cone on a dark background, when a beam of light passes through an optically inhomogeneous medium.

2.4.3. Study of Sorption Properties of TEG–Bentonite Composite

A total of 2 g of the TEG–bentonite composite were added to a liquid sample (100 mL) requiring purification, placed in a 250 mL beaker, and the mixture was stirred for 30–40 min at a temperature of 18 ± 5 °C, then left for 1 h, after which the phases were separated by filtration through a filter for finely dispersed sediments.

After purification of the model solution, the COD index and the content of cesium, strontium, cobalt, and manganese were measured. After purification of the RCW, radiometric measurements of the liquid phase were carried out.

2.4.4. Further Purification of Filtrate

A total of 0.5 g of a sorbent based on iron (III) hydroxide/oxide nanoparticles modified with nickel-potassium ferrocyanide was added to the filtrate (100 mL) from the experiments described in Section 2.4.3, placed in a 250 mL beaker, stirred for 1 h at a temperature of 18 ± 5 °C, then left for 1 h, after which the phases were separated by filtration through a filter for finely dispersed sediments. The synthesis of this sorbent is described in Zabulonov et al. [40] and references within. Ferrocyanides of different metals have a unique feature of possessing a high affinity with cesium ions [41].

3. Results and Discussion

3.1. Characterization of the Nano-Functionalized Composite Based on Bentonite and Magnetically Responsive TEG

One of the components of the nano-functionalized composite is magnetically responsive, thermally expanded graphite. Its characteristics and production method were previously described by Kadoshnikov et al. [19]; as a result of thermal shock, the intercalated graphite separates into lamellas due to the intense transition of intercalated graphite between graphite spheres to the gas phase. This forms a magnetically responsive TEG: Figure 1 shows an SEM micrograph of magnetically responsive TEG.

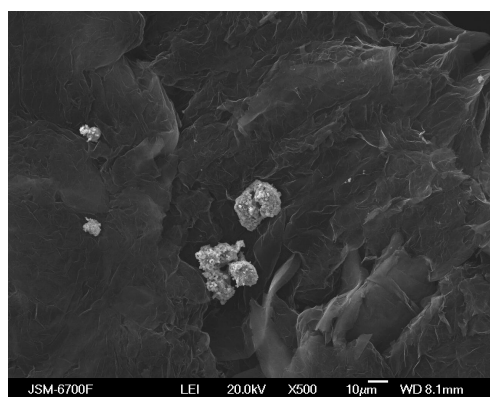


Figure 1. SEM micrograph of magnetically responsive thermally expanded graphite: magnification $\times 500$.

As can be seen from the figure, aggregates of spherical micro- and nanoparticles of iron/iron oxide are firmly fixed on the surface of the carbon matrix lamellae. This bond was established by the penetration of iron-containing particles between the graphite nanolayer flakes and the formation of iron carbides at a high temperature under microwave treatment conditions [42]. The formation of iron carbides is confirmed by X-ray diffractometry data, presented in the article by Kadoshnikov et al. [19]. The magnetoresponsive TEG nanosorbent retained high sorption capacity of the TEG matrix due to the presence of the active centers of oxidized graphene formed on the graphite surface under the conditions of the thermal oxidation shock [43]. The magnetoresponsive TEG is characterized by a low bulk density ($\sim 8 \text{ kg/m}^3$) and an increased bond strength between the magnetoresponsive component and the carbon matrix.

The second component of the nano-functionalized composite is the bentonite clay (Figure 2).

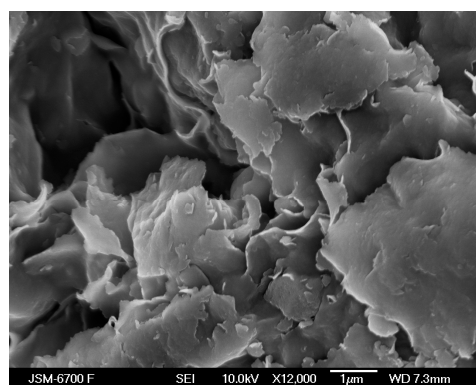
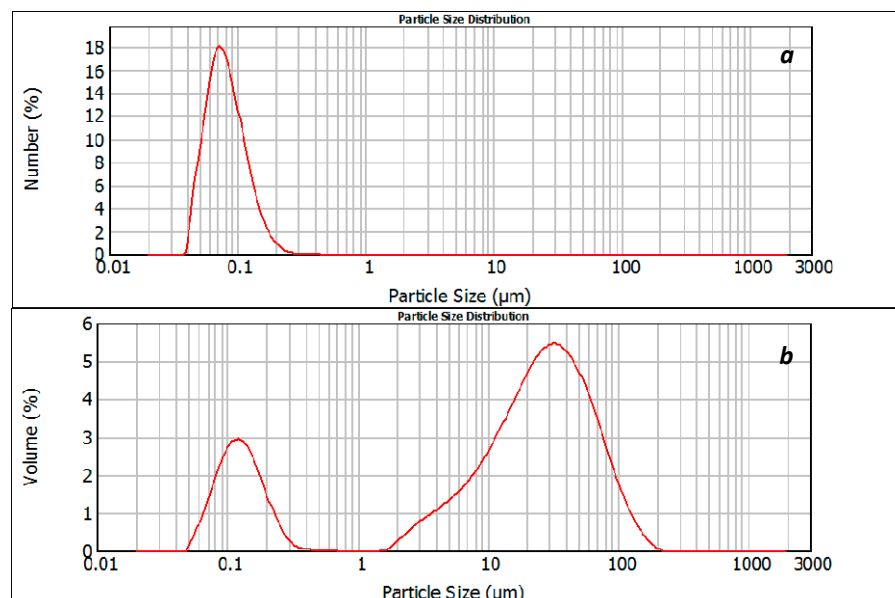


Figure 2. SEM micrograph of bentonite: magnification $\times 12,000$.

The use of bentonite in the TEG–bentonite composite promotes the sorption of polar organic substances due to its high hydrophilicity. Its main constituent montmorillonite has active sorption centers represented by aluminol and silanol groups, as well as the surface charge due to isomorphic substitutions in the crystal structure. These centers increase the sorption capacity of the clay component towards metal ions. The sorption activity of bentonite is significantly affected by the size of its particles and their aggregates. Table 1 shows the granulometric composition, and Figure 3 shows the differential distribution curves of bentonite particles.

Table 1. Granulometric composition (%) of bentonite from the Cherkasy deposit.

Fraction, μm	<1	1–10	10–100	>100
Sample, %	20.26	13.46	62.70	3.58

**Figure 3.** Differential distribution curves: by the number (a) and volume (b) of bentonite particles.

The dominant particle size of the sample (over 60%) is $\leq 100 \mu\text{m}$ (Figure 3).

To obtain a nano-functionalized magnetic carbon composite, the bentonite clay was mixed with the magnetically responsive, thermally expanded graphite, followed by mechanical activation of the mixture, as described in Section 2.2. The schematic for obtaining the magnetically responsive TEG–bentonite composite is summarized in Figure 4.

Hydrophilic centers are located on the surface edges and lateral parts of the peripheral areas of nanocrystals. They are provided mainly by silanol and aluminol centers, as well as negative charges. In addition, the bentonite montmorillonite particles (Figure 2) have hydrophobic sites. Over the course of mechanical mixing and activation, the hydrophobic smectite centers interact with the surfaces of TEG particles, which leads to the formation of loose aggregates that are capable of sorbing particles of micro- and nanoplastics and nonpolar hydrocarbons such as oil and surfactants with hydrophobic tails. The high affinity of bentonite particles with iron oxides facilitates the formation of a more homogeneous composite. In this composite, the montmorillonite particles interact with other components via van der Waals forces between the most hydrophobic surface areas, predominantly localized on the surface of the magnetically responsive TEG. This interaction results in the formation of aggregates, which increase homogeneity. In the process of coagulation, the hydrophilic centers play the most important role, as they are present in significantly larger numbers than hydrophobic sites in smectites [44].

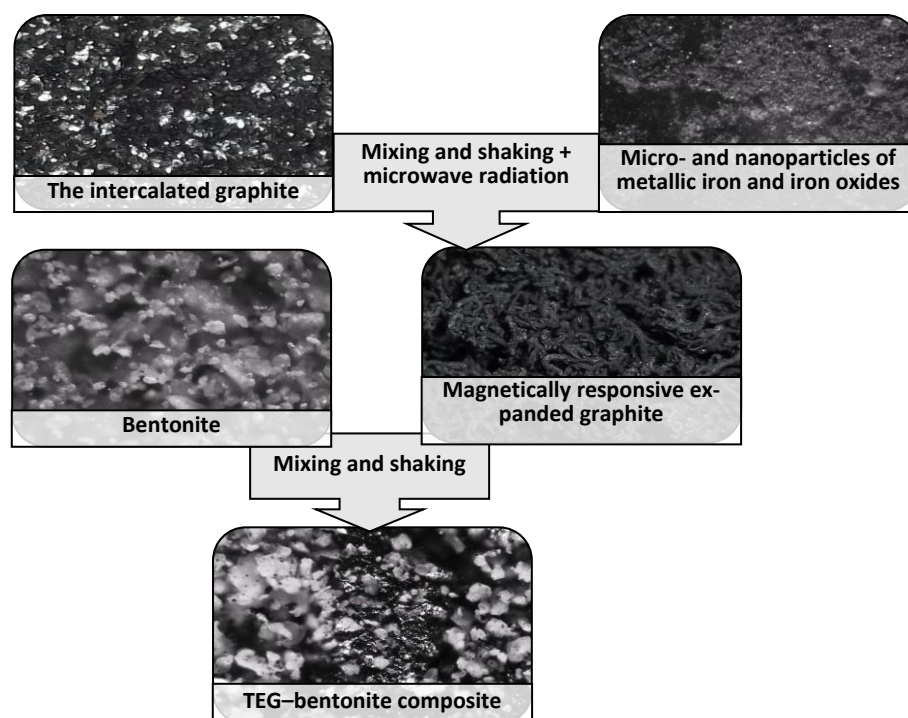


Figure 4. Schematic for obtaining magnetically responsive TEG–bentonite composite.

The optical image of the TEG–bentonite composite in reflected light is shown in Figure 5.

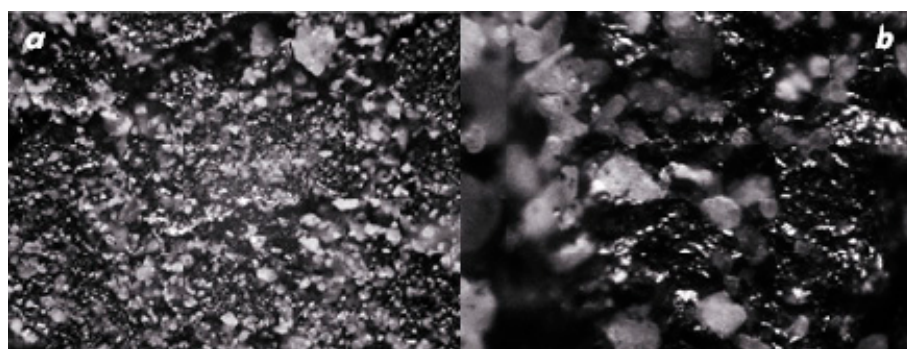


Figure 5. Photo of TEG–bentonite composite: (a) magnification $\times 50$; (b) magnification $\times 380$.

Mechanical activation can lead to the formation of surface defects. Micro- and macro-defects of the surface can create interference for the adsorption of molecules and introduce significant changes in the distribution of electrostatic and dispersion potential. In pores and cracks, there is a sharp increase in the dispersion potential. Dislocations emerging on the surface lead to the same effects, but their role, given the low concentrations, is small, and the transformations of the adsorption potential introduced by dislocations should only be taken into account at the early stages of filling the surface.

3.2. Study of Sorption Properties of the Obtained TEG–Bentonite Composite

3.2.1. Purification of NPP Radioactive Wastewater Simulant

The sorption properties of the obtained composite towards nonpolar hydrocarbons were assessed based on the results of determining the COD index of the simulant solution of NPP radioactive wastewaters, before and after treatment. The studies showed that the COD index, as a result of sorption treatment, decreased from 1500 to 135 mgO_2/dm^3 .

Cations of cesium, strontium, cobalt, and manganese were also removed from the solution (Figure 6).

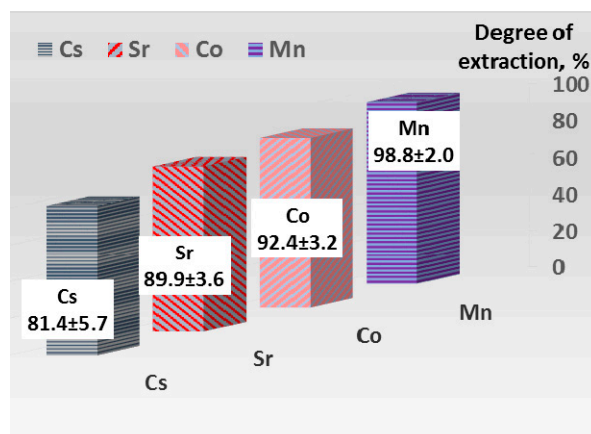


Figure 6. The degree of extraction of nonradioactive metal ions from the simulant solution of NPP radioactive wastewater by the TEG–bentonite composite.

The degree of extraction of cesium and strontium (81.4% and 89.9%, respectively) cannot be considered entirely satisfactory, in contrast to the degree of extraction of manganese (about 99%), which is explained by the competition of cations in the sorption process, as well as the formation of organomineral complex compounds that interfere with the sorption of cesium ions.

3.2.2. Purification of a Sample of Radioactively Contaminated Water (RCW)

The purification of real radioactively contaminated high-level water described in Section 2.4.2 was carried out in two stages. In the first stage, the contaminated water was treated with a TEG–bentonite composite according to the procedure described in Section 2.4.3. This treatment and subsequent phase separation resulted in the formation of a precipitate and a clear filtrate, free of solid particles, including colloidal particles, as confirmed by the absence of the Tyndall effect (Stage 1 of the purification process is shown in Figure 7). The high-level precipitate consists of magnetically responsive aggregates, formed during the heterocoagulation of micro- and nanoparticles of organic matter, including microplastics and hydrocarbons, with composite particles. Radionuclides adsorbed on the surface of micro-/nanoparticles also pass into the solid phase.

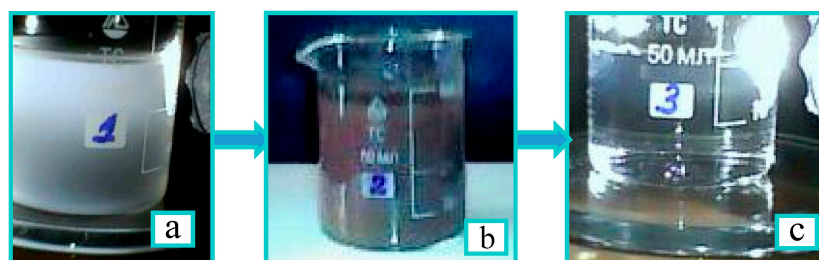


Figure 7. Stage 1 of the radioactively contaminated water purification process: (a) the original radioactively contaminated water; (b) TEG–bentonite composite decontamination; (c) purified water.

Sorption of non-polar hydrocarbons and nanoplastics was due to the presence of sorption centers localized mainly on the surface of the carbon component of the TEG–bentonite composite, while hydrophilic organic substances, as well as radionuclides, were sorbed mainly on the lateral faces of the montmorillonite microcrystals. At this stage, cesium and strontium were partially removed (Table 2). The multivalent radionuclides of Am-241 and

Eu-154 were removed completely, as they could not be detected in the filtrate. This is not surprising, considering that, firstly, multivalent cations are usually better adsorbed than mono- and divalent cations and, secondly, the initial chemical concentration of Am-241 and Eu-154 in the radioactive water sample was negligible (Table 3). At the second stage, for additional purification of the filtrate already free from colloid and suspended particles and containing water-soluble forms of radionuclides, a selective sorbent based on micro- and nanoparticles of iron hydroxide modified with nickel-potassium ferrocyanide by precipitation was used, which made it possible to decontaminate radioactively contaminated water (RCW) with an overall efficiency of 99.99%. The results of measuring the gamma and beta activity of the filtrates showed that the activity of cesium-137 and strontium-90 in the filtrate after the first stage of purification decreased by approximately three orders of magnitude—that is, the main fraction of the radionuclides was concentrated in the sediment—and at the second stage, the radionuclides that remained in the solution in the ionic form were sorbed (Table 2).

Table 2. Radioactivity of RCW. Sample volume 20 mL.

Processing Stage	Sorbent Used	Radionuclide	Activity, Bq/dm ³
Before (initial)	none	¹³⁷ Cs	3.3×10^7
		⁹⁰ Sr	4.9×10^6
After stage 1	TEG–bentonite composite	¹³⁷ Cs	$(7.50 \pm 0.31) \times 10^3$
		⁹⁰ Sr	$(1.83 \pm 0.28) \times 10^3$
After stage 2	Iron hydroxide with nickel–potassium ferrocyanide	¹³⁷ Cs	$(2.24 \pm 0.48) \times 10^2$
		⁹⁰ Sr	$(2.11 \pm 0.52) \times 10^2$

Table 3. Chemical concentration of radionuclides in the radioactive wastewater sample, before and after treatment.

Radionuclide	Initial Activity, Bq/dm ³	Specific Activity, Bq/g *	Initial Concentration, µg/dm ³	Concentration in RCW, µg/dm ³	
				After First Treatment	After Second Treatment
¹³⁷ Cs	3.3×10^7	3.2×10^{12}	10	2.4×10^{-3}	0.7×10^{-4}
⁹⁰ Sr	4.9×10^6	5.1×10^{12}	0.96	0.36×10^{-3}	0.4×10^{-4}
¹⁵⁴ Eu	2.4×10^3	1.0×10^{12} **	2.4×10^{-3}	not detected	not detected
²⁴¹ Am	2.2×10^4	1.27×10^{11}	0.17	not detected	not detected

* From [45]. ** Calculated from the half-life of ¹⁵⁴Eu = 8.6 y, as per [45].

The adsorption capacity of the sorbents used at stages 1 and 2 and in the treatment of the stimulant solution was rather different. For example, the TEG–bentonite composite adsorbed 0.415 mg Cs/g in the stimulant solution and only 0.5 µg/g from radioactive wastewater. However, such a comparison is not valid because the initial concentration of Cs in the former was 10.2 mg/dm³ and 10 µg/dm³ in the latter. The ratio between the initial concentrations, which is 1020:1, is not dissimilar to the ratio between the sorption capacities, which is 830:1. This might suggest the linear relationship between the sorption capacity and the concentration of the adsorbate at very low concentrations. The capacity of the ferrocyanide sorbent used at stage 2 for Cs was 4.6×10^{-4} µg/g.

4. Conclusions

1. A nano-functionalized magnetic carbon composite has been developed for the purification of multiphase and multicomponent man-made contaminated waters, simulta-

neously containing oil products, micro- and nanoplastics, and radionuclides and/or heavy metals. The composite is a mechanically activated mixture of bentonite and magnetically responsive, thermally expanded graphite, containing micro- and nanoparticles of iron and its oxides.

2. The sorption properties of the nano-functionalized magnetic carbon composite are due to active centers, mainly located on the surface of the oxidized graphene layers in thermally expanded graphite and on the outer surface of montmorillonite nanocrystals.

3. The use of the TEG–bentonite composite for the purification of water simulating radioactive contamination from a nuclear power plant (NPP) reduced the content of organic substances by 10–15 times, and the degree of extraction of cesium, strontium, cobalt, and manganese was from 81.4% to 99%.

4. The use of the TEG–bentonite composite for purification of real radioactively contaminated water with high activity, containing organic substances, including micro- and nanoplastics, reduced the radioactivity by three orders of magnitude. The use of cesium-selective sorbents for additional purification of the filtrate allowed for further decontamination of radioactively contaminated water, with an efficiency of 99.99%.

Author Contributions: Conceptualization, Y.L.Z. and V.M.K.; methodology, V.M.K. and T.I.M.; formal analysis, T.I.N., I.V.M. and O.M.A.; data analysis, Y.L.Z., S.V.M. and V.M.K.; resources, Y.L.Z.; data curation, L.A.O.; writing—original draft preparation, V.M.K. and T.I.M.; writing—review and editing, V.M.K., T.I.M., S.V.M. and O.M.A.; supervision, Y.L.Z.; project administration, Y.L.Z. All authors have read and agreed to the published version of the manuscript.

Funding: The project was funded by the State Institution “The Institute of Environmental Geochemistry of National Academy of Sciences of Ukraine”, and the contribution of the European Union’s project CLEANWATER, grant agreement 101131382, is also acknowledged. S.V.M. was supported by the UKRI (UK Research and Innovation) project-EP/Y037154/1.

Institutional Review Board Statement: Not applicable.

Data Availability Statement: The original contributions presented in this study are included in the article. Further inquiries can be directed to the corresponding author.

Acknowledgments: The authors express their sincere gratitude to V.Y-E. Khan, the Radiation Monitoring Department, and O.O. Odintsov, the Sector of Physicochemical Methods of Analysis of the Institute for Safety Problems of Nuclear Power Plants, National Academy of Sciences of Ukraine, for help with radioactivity measurements and participation in the discussion of the results.

Conflicts of Interest: Author Sergey V. Mikhalovsky was employed by Advanced Nanostructured Materials Design and Consultancy (ANAMAD) Ltd. The remaining authors declare that the research was conducted in the absence of any commercial or financial relationships that could be construed as a potential conflict of interest.

References

1. Strokai, V.; Kuiper, E.J.; Bak, M.P.; Vriend, P.; Wang, M.; van Wijnen, J.; Strokai, M. Future microplastics in the black Sea: River exports and reduction options for zero pollution. *Mar. Pollut. Bull.* **2022**, *178*, 113633. [[CrossRef](#)] [[PubMed](#)]
2. Kivva, S.; Zheleznyak, M.; Bezhenar, R.; Pylypenko, O.; Sorokin, M.; Demydenko, A.; Kanivets, V.; Laptev, G.; Votsekhovich, O.; Boyko, V.; et al. Modeling of major environmental risks for the Kyiv city, Ukraine from the Dnieper river waters-inundation of coastal areas and contamination by the radionuclides deposited in bottom sediments after the Chernobyl accident. In Proceedings of the EGU General Assembly 2021, Online, 19–30 April 2021; EGU21-13038. [[CrossRef](#)]
3. Shumilova, O.; Sukhodolov, A.; Osadcha, N.; Oreshchenko, A.; Constantinescu, G.; Afanasyev, S.; Koken, M.; Osadchyi, V.; Rhoads, B.; Tockner, K.; et al. Environmental effects of the Kakhovka Dam destruction by warfare in Ukraine. *Science* **2025**, *387*, 1181–1186. [[CrossRef](#)]
4. Zub, L.; Prokopuk, M.; Netsvetov, M.; Gudkov, D. Does long-term radiation exposure in Chernobyl impact the reproductive structures of *Nuphar lutea* (Linn’*e*) Smith? *Environ. Pollut.* **2024**, *363*, 125067. [[CrossRef](#)] [[PubMed](#)]

5. Rajkhowa, S.; Sarma, J.; Rani Das, A. Chapter 15. Radiological contaminants in water: Pollution, health risk, and treatment. In *Contamination of Water*; Elsevier: Amsterdam, The Netherlands, 2021; pp. 217–236. [\[CrossRef\]](#)
6. Abdel Rahman, R.O.; Ibrahim, H.A.; Hung, Y.-T. Liquid radioactive wastes treatment: A review. *Water* **2011**, *3*, 551–565. [\[CrossRef\]](#)
7. Gossard, A.; Lilin, A.; Faure, S. Gels, coatings and foams for radioactive surface decontamination: State of the art and challenges for the nuclear industry. *Prog. Nucl. Energy* **2022**, *149*, 104255. [\[CrossRef\]](#)
8. Rudenko, L.I.; Khan, V.E.; Kashkovskiy, V.I.; Dzhuzha, O.V. Purification of drain water and distillation residue from organic compounds, transuranic elements, and uranium at the Chornobyl NPP. *Sci. Innov.* **2014**, *10*, 16–25. [\[CrossRef\]](#)
9. Smith, M.; Love, D.C.; Rochman, C.M.; Neff, R.A. Microplastics in seafood and the implications for human health. *Curr. Environ. Health Rep.* **2018**, *5*, 375–386. [\[CrossRef\]](#)
10. Khan, A.; Jia, Z. Recent insights into uptake, toxicity, and molecular targets of microplastics and nanoplastics relevant to human health impacts. *IScience* **2023**, *26*, 106061. [\[CrossRef\]](#) [\[PubMed\]](#)
11. Li, C.; Zhou, Z.; Meng, X.; Li, J.; Chen, H.; Yu, T.; Xu, M. A preliminary study on the “hitchhiking” of radionuclides on microplastics: A new threat to the marine environment from compound pollution. *Toxics* **2025**, *13*, 429. [\[CrossRef\]](#)
12. Li, C.; Zhou, Z.; Li, J.; Huang, F.; Zhu, X.; Gao, F.; Yu, T.; Hu, M. Marine microplastics fuel long-range transport of radioactive nuclides: A review. *Mar. Pollut. Bull.* **2025**, *221*, 118540. [\[CrossRef\]](#)
13. Yang, M.; Zhang, B.; Xin, X.; Lee, K.; Chen, B. Microplastic and oil pollution in oceans: Interactions and environmental impacts. *Sci. Total Environ.* **2022**, *838*, 156142. [\[CrossRef\]](#)
14. Lin, Z.; Hu, X.; Lin, H.; Yu, G.; Shen, L.; Yu, W.; Li, B.; Leihong, Z.; Ying, M. Membrane technology for microplastic removal: Microplastic occurrence, challenges, and innovations of process and materials. *Chem. Eng. J.* **2025**, *520*, 166183. [\[CrossRef\]](#)
15. Topuz, F.; Abdulhamid, M.A. Tailored nanofibrous polyimide-based membranes for highly effective oil spill cleanup in marine ecosystems. *Chemosphere* **2024**, *368*, 143730. [\[CrossRef\]](#)
16. de Rosset, A.; Torres-Mendieta, R.; Pasternak, G.; Yalcinkaya, F. Synergistic effects of natural biosurfactant and metal oxides modification on PVDF nanofiber filters for efficient microplastic and oil removal. *Process Saf. Environ. Prot.* **2020**, *194*, 997–1009. [\[CrossRef\]](#)
17. Hummers, W.S.; Offeman, R.E. Preparation of graphitic oxide. *J. Am. Chem. Soc.* **1958**, *80*, 1339. [\[CrossRef\]](#)
18. Feicht, P.; Biskupek, J.; Gorelik, T.E.; Renner, J.; Halbig, C.E.; Maranska, M.; Puchter, F.; Kaiser, U.; Eigler, S. Brodie’s or Hummers’ method: Oxidation conditions determine the structure of graphene oxide. *Chem. Eur. J.* **2019**, *25*, 8955–8959. [\[CrossRef\]](#)
19. Kadoshnikov, V.M.; Melnychenko, T.I.; Arkhipenko, O.M.; Tutsykyi, D.H.; Komarov, V.O.; Bulavin, L.A.; Zabulonov, Y.L. A composite magnetosensitive sorbent based on the expanded graphite for the clean-up of oil spills: Synthesis and structural properties. *C* **2023**, *9*, 39. [\[CrossRef\]](#)
20. Coetzee, D.; Rojviroon, T.; Niamlang, S.; Militký, J.; Wiener, J.; Večerník, J.; Melicheríková, J.; Müllerová, J. Effects of expanded graphite’s structural and elemental characteristics on its oil and heavy metal sorption properties. *Sci. Rep.* **2024**, *14*, 13716. [\[CrossRef\]](#)
21. Zhang, Q.; Bi, T.; Chen, H.; Hu, Y.; Tian, F.; Lin, Q. Petroleum residue-based ultrathin-wall graphitized mesoporous carbon and its high-efficiency adsorption mechanism. *Diam. Relat. Mater.* **2024**, *148*, 111497. [\[CrossRef\]](#)
22. Eigler, S.; Dotzer, C.; Hof, F.; Bauer, W.; Hirsch, A. Sulfur species in graphene oxide. *Chem. Eur. J.* **2013**, *19*, 9490–9496. [\[CrossRef\]](#)
23. Amirov, R.R.; Shayimova, J.; Nasirova, Z.; Solodov, A.; Dimiev, A.M. Analysis of competitive binding of several metal cations by graphene oxide reveals the quantity and spatial distribution of carboxyl groups on its surface. *Phys. Chem. Chem. Phys.* **2018**, *20*, 2320–2329. [\[CrossRef\]](#)
24. Schiffman, P.; Southard, R.J. Cation exchange capacity of layer silicates and palagonitized glass in mafic volcanic rocks: A comparative study of bulk extraction and in situ techniques. *Clays Clay Min.* **1996**, *44*, 624–634. [\[CrossRef\]](#)
25. Liu, H.; Fu, T.; Sarwar, M.T.; Huaming Yang, H. Recent progress in radionuclides adsorption by bentonite-based materials as ideal adsorbents and buffer/backfill materials. *Appl. Clay Sci.* **2023**, *232*, 106796. [\[CrossRef\]](#)
26. Uddin, F. Ch 1: Montmorillonite: An introduction to properties and utilization. In *Current Topics in the Utilization of Clay in Industrial and Medical Applications*; Zoveidavianpoor, M., Ed.; IntechOpen: London, UK, 2018; pp. 3–23, ISBN 978-1-78923-729-0. [\[CrossRef\]](#)
27. İnan, S. Inorganic ion exchangers for strontium removal from radioactive waste: A review. *J. Radioanal. Nucl. Chem.* **2022**, *331*, 1137–1154. [\[CrossRef\]](#)
28. Saleh, A.S.; Afolabi, O.O. Enhancement and modelling of caesium and strontium adsorption behaviour on natural and activated bentonite. *Environ. Technol. Innov.* **2025**, *37*, 103937. [\[CrossRef\]](#)
29. Muslim, W.A.; Al-Nasri, S.K.; Albayati, T.M.; Salih, I.K. Investigation of bentonite clay minerals as a natural adsorbents for Cs-137 real radioactive wastewater treatment. *Desalination Water Treat.* **2024**, *317*, 100121. [\[CrossRef\]](#)
30. Khodakov, G.S. *Fizikaizmel’Cheniya (Physics of Comminution in Russian)*; Nauka Publ.: Moscow, Russia, 1972; UDK 532.6.

31. Zabashta, Y.F.; Kovalchuk, V.I.; Svechnikova, O.S.; Bulavin, L.A. Electrocapillary properties of hydrogels. *Ukr. J. Phys.* **2022**, *67*, 658–662. [CrossRef]
32. Esmaeili, E.; Rounaghi, S.A.; Eckert, J. Mechanochemical synthesis of rosin-modified montmorillonite: A breakthrough approach to the next generation of OMMT/rubber nanocomposites. *Nanomaterials* **2021**, *11*, 1974. [CrossRef]
33. Yudina, T.F.; Ershova, T.V.; Beylina, N.Y.; Smirnov, N.N.; Bratkov, I.V.; Shchennikov, D.V. Mechanochemical activation of graphite materials. *News of Higher Educational Institutions. Chemistry and Chemical Technology*, 2012; p. 55, line 29–33.
34. Smirnova, D.N.; Grishin, I.S.; Smirnov, N.N. Synthesis, structure and properties of bentonite-activated carbon composite. *ChemChemTech* **2024**, *67*, 59–66. [CrossRef]
35. Yashkova, D.; Grishin, I.; Smirnov, N. Mechanism of tetracycline sorption on carbon-bentonite. *Chem. Towards Technol. Step-By-Step* **2024**, *5*, 54–60. [CrossRef]
36. Nasiedkin, D.B.; Grebenyuk, A.G.; Babich, I.V.; Plyuto, Y.V.; Kartel, M.T. Experimental and theoretical study on expanded graphite oxidation. *Surface* **2015**, *7*, 126–136; UDK 543.573.
37. Boichenko, S.; Lejda, K.; Mateichyk, V.; Topilnytskyi, P. *Problems of Chemmotology. Theory and Practice of Rational Use of Traditional and Alternative Fuels & Lubricants: Monograph*; Center of Educational Literature: Kyiv, Ukraine, 2017; pp. 136–141, ISBN 978-617-673-632-5.
38. ISO 15705: 2002; Water Quality: Determination of the Chemical Oxygen Demand Index (ST-COD)-Small-Scale Sealed-Tube Method. International Standardisation Organisation: Geneva, Switzerland, 2002.
39. Rudenko, L.I.; Gumenna, O.A.; Dzhuzha, O.V. Membrane methods of treatment of water, which contains polymeric substances and compounds of uranium, strontium, and sodium. *Rep. Natl. Acad. Sci. Ukr.* **2010**, *6*, 134–138.
40. Zabulonov, Y.; Melnychenko, T.; Kadoshnikov, V.; Kuzenko, S.; Guzii, S.; Peer, I. New sorbents and their application for deactivation of liquid radioactive waste. In *Liquid Radioactive Waste Treatment: Ukrainian Context*; LWRT 2022; Lecture Notes in Civil Engineering; Zabulonov, Y., Peer, I., Zheleznyak, M., Eds.; Springer: Cham, Switzerland, 2024; Volume 469, pp. 126–136. [CrossRef]
41. Toropov, A.S.; Satayeva, A.R.; Mikhalovsky, S.; Cundy, A.B. The use of composite ferrocyanide materials for treatment of high salinity liquid radioactive wastes rich in cesium isotopes. *Radiochim. Acta* **2014**, *102*, 911–917. [CrossRef]
42. Sun, M.M.; Zhang, J.L.; Li, K.J.; Ren, S.; Wang, Z.M.; Jiang, C.H.; Li, H.T. Dissolution behaviors of various carbonaceous materials in liquid iron: Interaction between graphite and iron. *JOM* **2019**, *12*, 4305–4310. [CrossRef]
43. Dimiev, A.M.; Shukhina, K.; Khannanov, A. Mechanism of the graphene oxide formation: The role of water, “reversibility” of the oxidation, and mobility of the C–O bonds. *Carbon* **2020**, *166*, 1–14. [CrossRef]
44. Zabulonov, Y.L.; Melnychenko, T.I.; Kadoshnikov, V.M.; Odukalets, L.A.; Kuzenko, S.V. A Method for Producing a Magnetically Sensitive Nanocomposite for the Purification of Technologically Contaminated and Radioactive Waters Containing Micro- and Nanoplastics and Oil Products. *UA156277U*. 2024. Available online: <https://sis.nipo.gov.ua/uk/search/detail/1801151/> (accessed on 18 August 2025). (In Ukrainian)
45. Determining the Mass Related Activity of Radionuclides. ÄQUIVAL/MASSAKT-01. Procedures Manual for Monitoring of Radioactive Substances in the Environment and of External Radiation. 2022. ISSN 1865-8725. Available online: https://www.bmu.de/fileadmin/Daten_BMU/Download_PDF/Strahlenschutz/Messanleitungen_2022/aequival_massakt_v2022-03_en_bf.pdf (accessed on 20 August 2025).

Disclaimer/Publisher’s Note: The statements, opinions and data contained in all publications are solely those of the individual author(s) and contributor(s) and not of MDPI and/or the editor(s). MDPI and/or the editor(s) disclaim responsibility for any injury to people or property resulting from any ideas, methods, instructions or products referred to in the content.